IEEE Access
Multidisciplinary | Rapid Review | Open Access Journal

Received February 24, 2021, accepted March 6, 2021, date of publication March 18, 2021, date of current version March 30, 2021.

Digital Object Identifier 10.1109/ACCESS.2021.3067038

Improved Adaptive Integral-Sliding-Mode Fault-Tolerant Control for Hypersonic Vehicle With Actuator Fault

FUHUI GUO AND PINGLI LU
School of Automation, Beijing Institute of Technology, Beijing 100081, China
Corresponding author: Pingli Lu (pinglilu@bit.edu.cn)

This work was supported by the National Science Foundation of China under Grant 61433003, Grant 60904003, and Grant 11602019.

ABSTRACT In this paper, the problem of attitude control for hypersonic vehicle in the present of actuator fault and unknown uncertainties including modeling uncertainties, aerodynamic parameters uncertainties is investigated based on integral sliding mode technique. A fault-tolerant control (FTC) law is proposed consisting of three parts, an improved integral sliding mode(ISM) equivalent control law, a power reaching law and a new adaptive compensation control law. The proposed FTC possesses triple advantages. Firstly, when sliding mode is established, the proposed equivalent controller will offer faster convergence speed via introducing a switching condition into the conventional ISM control. Secondly, the adaptive compensation control law is presented considering both the unknown uncertainty and the unexpected actuator fault including additive fault and multiplicative fault. Finally, the boundness of bounded unknown uncertainty is no longer needed in advance. Simulation results show the effectiveness and the superiority of the proposed fault-tolerant controller on fast convergence speed and expected attitude tracking performance.

INDEX TERMS Actuator failure, attitude control, fault-tolerant control, hypersonic vehicle, integral sliding mode.

I. INTRODUCTION

Hypersonic vehicle (HSV) has attracted plenty of interest among many researchers around the world due to its especial superiority in quick maneuverability and large flight envelope. Therefore many issues around HSV have become popular, especially, attitude control for HSV. For decades, various researches on HSV have been developed [1]–[7]. As we know, modeling uncertainties and ever-changing external environment bring huge difficulty for controller design. Meanwhile, complex flight conditions and aging components of flight system often lead to multiple faults, such as actuator failure, sensor failure and system failure [8]–[16]. All these failures may lead to stability reduction, system performance deterioration and security breach of the HSV closed-loop system, and in case of serious failure, catastrophic accidents are inevitable. Hence, fault-tolerant control for HSV in the present of single and multiple faults has become a research hotspot in recent years [17]–[22].

The associate editor coordinating the review of this manuscript and approving it for publication was Ning Sun.

To the best of our knowledge, there are two major issues on FTC design for HSV. Firstly, among all types of HSV faults, actuator fault has attracted most attention due to its high occurrence probability. Moreover, the vast majority of theoretical research and simulation experiment on actuator faults refer to either addictive faults or multiplicative faults [42]–[44]. Hence the first challenge is to handle multiple faults simultaneously. In addition, it is hardly to predict the fault type, time of fault occurrence and the degree of fault. As a result, specific information of fault is always difficult to obtain in the realistic flight process. Then the second challenge can be summarised, that is, how to design the fault-tolerant controller with minimal fault information or without requirement on specific fault to be known a priori.

For decades, many control methods have been involved for fault-tolerant controller design for HSV [23]–[30]. Jiang *et al.* [23] designed the back-stepping controller combined with neural network observer to reconfigure flight controller, when control effector damaged. However, the remarkable draw of back-stepping method is the 'explosion of complexity'. Then Qi *et al.* [24] introduced a dynamic surface strategy into the back-stepping method to eliminate

the unexpected feature. Also, Qi *et al.* [24] applied the method to longitude control for hypersonic vehicle with faulty redundant elevators. In [25] and [26], model predictive control was adopted to cope with actuator saturation for HSV. Meanwhile, plenty of research results are based on sliding mode control (SMC) technique. In [27] an integral sliding mode control strategy was investigated to design a fault-tolerant controller for air-breathing supersonic missiles, even in the presence of actuator faults. Zhai *et al.* [28] dealt with the unknown additive fault causing by unknown actuator failure of HSV.

Among various control strategies, sliding mode control stays ahead of others due to its easy implementation and insensitivity to unknown uncertainty. Therefore, many researchers focus on fault-tolerant control for HSV on the basis of SMC, such as linear sliding mode control (LSMC), integral sliding mode control(ISMC), terminal sliding mode (TSMC) and high order sliding mode control (HOSMC) [31]–[39]. However, linear sliding mode control can only guarantee the asymptotic convergence of system states and ISMC, TSMC and HOSMC perform better in their finite-time converge. Sun *et al.* [31], [32] have utilized ISMC to design finite-time controller for HSV. Moreover, in [32], integral sliding mode strategy was employed to tracking-control issue for HSV with actuator failure. As a result, the tracking errors of velocity and altitude converged in finite time. Yet, when initial location of the system states departs far from the equilibrium point, the actual convergence speed of the system states is not entirely satisfactory. Thus, Ding *et al.* [33] investigated a fast integral sliding mode control law by simplifying the adjustment process of coefficients. In addition, terminal sliding mode control is another finite-time SMC and is also popular among many researchers [34]–[36]. In [34] a passive fault-tolerant control strategy was proposed based on adaptive TSMC. However, the establishment of terminal sliding mode results in the singularity of TSMC. Therefore Liang *et al.* [35] designed a non-singular TSMC to avoid the drawback and improve the attitude tracking performance. Besides, high-order sliding mode is also an effective control method and always combines with integral sliding and terminal sliding mode [36]–[39]. In [36] and [37], high-order sliding mode technique combined with integral sliding mode was adopted to design attitude controller for HSV and velocity-altitude controller for air-breathing hypersonic vehicle, respectively by Zong *et al.* However, the convergence speed of system states of closed-loop under high-order sliding mode controller is not always gratifying.

Inspired by the above discussion, an improved adaptive integral sliding mode fault-tolerant controller is proposed with three advantages. Firstly, inspired by [38] and [39], a switching condition is introduced into conventional integral sliding mode control in absence of uncertainties and faults to accelerate the respond speed of system. In [38], 'unit circle' is selected as a rational to improve the transient process. Different from [38], a new switching condition is proposed in this paper. It offers a more precise range on the basis of actual system states. Moreover, compared with [39], no additional parameters are required. Secondly, both the additive fault and multiplicative fault are considered. Thirdly, actuator faults are treated as a kind of unknown disturbance. Then the uncertainties include modeling uncertainties, external disturbance and unknown actuator faults. Moreover, the proposed controller considers the fact that the bounds of the uncertainties are unknown before in controller design.

The reminder of this paper is organized as follows. The preliminaries and problem statement are given in Section II. The proposed controller is detailed in Section III. Section IV provides the numerical simulations to illustrate the effectiveness of the proposed method. Section V concludes the paper.

II. PROBLEM STATEMENT

A. NOTATIONS AND LEMMA

Notations : $\mathcal{R}^{m\times n}$ denote $m \times n$ matrix. $(\cdot)^T$ denotes the transpose of matrix $(\cdot)$. $(\cdot)^{-1}$ denotes the inverse of matrix $(\cdot)$. $\mathrm{sgn}(\cdot)$ is the sign function. $\lambda_{max}(\cdot)$ denotes the maximum eigenvalues of a matrix. $\lambda_{min}(\cdot)$ denotes the minimum eigenvalues of a matrix. For vector $\boldsymbol{o} = [o_1, o_2, \cdots, o_n]^T$ and real vector $\boldsymbol{\gamma} = [\gamma_1, \gamma_2, \cdots, \gamma_n]^T$, the following notations are defined. $\dot{\boldsymbol{o}} = [\dot{o}_1, \dot{o}_2, \cdots, \dot{o}_n]^T$. $\mathrm{diag}(\boldsymbol{o}) \in \mathcal{R}^{n\times n}$ represents a diagonal matrix composed of each elements in $\boldsymbol{o}$. $\boldsymbol{o}^{\boldsymbol{\gamma}} = [o_1^{\gamma_1}, o_2^{\gamma_2}, \cdots, o_n^{\gamma_n}]^T$. $sig^{\gamma_i}(o_i) = |o_i|^{\gamma_i}\mathrm{sgn}(o_i)$. $\int_0^t sig^{\gamma_i}(o_i)d\tau = \int_0^t |o_i(\tau)|^{\gamma_i}\mathrm{sgn}(o_i(\tau))d\tau$. $\boldsymbol{sig}^{\boldsymbol{\gamma}}(\boldsymbol{o}) = [sig^{\gamma_1}(o_1), sig^{\gamma_2}(o_2), \cdots, sig^{\gamma_n}(o_n)]^T$. $\int_0^t \boldsymbol{sig}^{\boldsymbol{\gamma}}(\boldsymbol{o}(\iota))d\iota = \left[\int_0^t sig^{\gamma_1}(o_1)d\iota, \int_0^t sig^{\gamma_2}(o_2)d\iota, \ldots, \int_0^t sig^{\gamma_n}(o_n)d\iota\right]^T$.

Lemma 1 ([40]): Let $k_i > 0 (i = 1, 2, 3)$, such that the polynomial $\lambda^3 + k_3\lambda^2 + k_2\lambda + k_1$ is Hurwitz. There exists $\epsilon \in (0, 1)$ such that the following double integral system

$$\begin{cases} \dot{o}_1 = o_2 \\ \dot{o}_2 = v \end{cases} \tag{1}$$

can be stabilized at the origin in finite time under the following controller

$$v = -k_1 sig^{a_1}(o_1) - k_2 sig^{a_2}(o_2) \tag{2}$$

with $a_1 = \frac{a_2 a_3}{2a_3 - a_2}$, $a_2 \in (1-\epsilon, 1)$ and $a_3 = 1$. In other words, the following equation holds.

$$o_1 = o_2 = 0 \tag{3}$$

Lemma 2 ([5]): There exists a positive constant $l (0 < l < 1)$ such that for $x_i \in \mathcal{R}^{n\times 1} (i = 1, \cdots, n)$, the following inequality holds.

$$(\sum_{i=1}^{n} |x_i|)^l \leq \sum_{i=1}^{n} |x_i|^l \leq n^{1-l}(\sum_{i=1}^{n} |x_i|)^l \tag{4}$$

B. MATHEMATIC MODEL AND CONTROL OBJECTIVE

The mathematic model of attitude dynamics of rigid-body hypersonic vehicle is formulated in the control-orient form

as follows [4]

$$\begin{cases} \dot{\alpha} &= q - p\tan\beta\cos\alpha + r\tan\beta\sin\alpha \\ \dot{\beta} &= p\sin\alpha - r\cos\alpha \\ \dot{\mu} &= p\sec\beta\cos\alpha + r\sec\beta\sin\alpha \\ \dot{p} &= \frac{I_{zz}}{I^*}M_x + \frac{I_{xz}}{I^*}M_z + I_{p1}pq + I_{p2}qr \\ \dot{q} &= \frac{1}{I_{yy}}M_y + I_{q1}(r^2 - p^2) + I_{q2}pr \\ \dot{r} &= \frac{I_{xz}}{I^*}M_x + \frac{I_{xx}}{I^*}M_z + I_{r1}pq + I_{r2}qr \end{cases} \tag{5}$$

where α, β, μ are angle of attack, side-slip angle and bank angle, respectively. p, q, r are the angular rate (roll, pitch, and yaw rates respectively). I_{xx}, I_{yy}, I_{zz} are the moment of inertia. I_{xz} is product of inertia. $I^* = I_{xx}I_{zz} - I_{xz}^2$. $I_{p1}, I_{p2}, I_{q1}, I_{q2}, I_{r1}, I_{r2}$ are formulated as below. $I_{p1} = ((I_{xx} - I_{yy} + I_{zz})I_{xz})/I^*$, $I_{p2} = ((I_{yy} - I_{zz})I_{zz} - I_{xz}^2)/I^*$, $I_{q1} = I_{xz}/I_{yy}$, $I_{q2} = (I_{zz} - I_{xx})/I_{yy}$, $I_{r1} = ((I_{xx} - I_{yy})I_{xx} + I_{xz}^2)/I^*$, $I_{r2} = ((-I_{xx} + I_{yy} - I_{zz})I_{xz})/I^*$.

Then (5) can be rewritten in the following form

$$\dot{\boldsymbol{x}}_1 = \boldsymbol{R}(\boldsymbol{x}_1)\boldsymbol{x}_2 + \boldsymbol{\Delta}_1 \tag{6}$$

$$\dot{\boldsymbol{x}}_2 = \boldsymbol{I}^{-1}(-\boldsymbol{x}_2^{\times}\boldsymbol{I}\boldsymbol{x}_2 + \boldsymbol{M} + \boldsymbol{\Delta}_2) \tag{7}$$

where $\boldsymbol{x}_1 = [\alpha, \beta, \mu]^T$ and $\boldsymbol{x}_2 = [p, q, r]^T$. $\boldsymbol{\Delta}_1 \in \mathcal{R}^{3\times 1}$ is unknown modeling uncertainties. Control input is $\boldsymbol{M} = [M_x, M_y, M_z]^T$. Inertia matrix $\boldsymbol{I}$, linear skew-symmetric matrix operator $\boldsymbol{x}_2^{\times}$ and coordinate-transformation matrix $\boldsymbol{R}(\boldsymbol{x}_1)$ are as follows

$$\boldsymbol{I} = \begin{bmatrix} I_{xx} & 0 & -I_{xz} \\ 0 & I_{yy} & 0 \\ -I_{xz} & 0 & I_{zz} \end{bmatrix}, \boldsymbol{x}_2^{\times} = \begin{bmatrix} 0 & -r & q \\ r & 0 & -p \\ -q & p & 0 \end{bmatrix} \text{ and}$$

$$\boldsymbol{R}(\boldsymbol{x}_1) = \begin{bmatrix} -\cos\alpha\tan\beta & 1 & -\sin\alpha\tan\beta \\ \sin\alpha & 0 & -\cos\alpha \\ -\cos\alpha\sec\beta & 0 & -\sin\alpha\sec\beta \end{bmatrix}.$$

$\boldsymbol{\Delta}_2 \in \mathcal{R}^{3\times 1}$ is unknown bounded external disturbance [5], [37]. Apart from the above unknown uncertainties, inertia uncertainty is also considered herein and formulated as $\Delta\boldsymbol{I}$, thus the inertia matrix $\boldsymbol{I}$ is rewritten as $\boldsymbol{I} = \boldsymbol{I}_n + \Delta\boldsymbol{I}$. $\boldsymbol{I}_n$ denotes the nominal inertia matrix. Then (7) turns to

$$\dot{\boldsymbol{x}}_2 = \boldsymbol{I}_n^{-1}(-\boldsymbol{x}_2^{\times}\boldsymbol{I}_n\boldsymbol{x}_2 + \boldsymbol{u}) + \boldsymbol{I}_n^{-1}(-\boldsymbol{x}_2^{\times}\Delta\boldsymbol{I}\boldsymbol{x}_2 - \Delta\boldsymbol{I}\dot{\boldsymbol{x}}_2 + \boldsymbol{\Delta}_2) \tag{8}$$

with $\boldsymbol{u} = \boldsymbol{M}$.

Generally, the deflection of aerodynamic surface brings control torque. Therefore, actuator fault is reflected by control torque $\boldsymbol{M}$ and the actuator fault discussed in this paper can be expressed as

$$\boldsymbol{u} = \boldsymbol{\Theta}\boldsymbol{u}_d + \boldsymbol{\rho} \tag{9}$$

with $\boldsymbol{u}_d = [u_{d1}, u_{d2}, u_{d3}]^T$ is the expected control input vector. $\boldsymbol{\Theta}$ is the actuator effectiveness matrix and $\boldsymbol{\Theta} = \text{diag}(\theta_1, \theta_2, \theta_3)$, $0 < \theta_i (i = 1, 2, 3) \leq 1$. If $\theta_i (i = 1, 2, 3) = 1$, it means the i^{th} actuator conducts normally, otherwise, i^{th} actuator works with failure. Additive fault is denoted by $\boldsymbol{\rho} = [\rho_1, \rho_2, \rho_3]^T$, $\underline{\rho} < |\rho_i (i = 1, 2, 3)| \leq \bar{\rho}$ ($\underline{\rho}$ and $\bar{\rho}$ are unknown positive constants). Therefore, the dynamic equation of attitude control system with inertia uncertainties, unknown external uncertainties and multiple-type actuator faults can be given by (6) and (8).

Fundamentally speaking, the attitude control objective is to force the aerodynamic angels $\boldsymbol{x}_1 = [\alpha, \beta, \mu]^T$ track the desired aerodynamic angels $\boldsymbol{x}_{1d} = [\alpha_d, \beta_d, \mu_d]^T$, which can be expressed as a tracking error vector $\boldsymbol{e} = [e_1, e_2, e_3]^T$,

$$\boldsymbol{e} = \boldsymbol{x}_1 - \boldsymbol{x}_{1d} \tag{10}$$

$$\dot{\boldsymbol{e}} = \dot{\boldsymbol{x}}_1 - \dot{\boldsymbol{x}}_{1d} \tag{11}$$

with $\|\dot{\boldsymbol{x}}_{1d}\| \leq \xi_{1d} (\xi_{1d} > 0)$. Define $\boldsymbol{z}_1 = \boldsymbol{e}$ and $\boldsymbol{z}_2 = \dot{\boldsymbol{z}}_1$, then a double integral system can be obtained,

$$\begin{cases} \dot{\boldsymbol{z}}_1 = \boldsymbol{z}_2 \\ \dot{\boldsymbol{z}}_2 = \ddot{\boldsymbol{x}}_1 - \ddot{\boldsymbol{x}}_{1d} \end{cases} \tag{12}$$

$\boldsymbol{z}_1 = [z_{11}, z_{12}, z_{13}]^T$ and $\boldsymbol{z}_2 = [z_{21}, z_{22}, z_{23}]^T$. The representation of $\ddot{\boldsymbol{x}}_1$ can be obtained by differentiating $\boldsymbol{x}_1$ twice,

$$\begin{aligned} \ddot{\boldsymbol{x}}_1 &= \frac{d}{dt}(\boldsymbol{R}(\boldsymbol{x}_1)\boldsymbol{x}_2 + \boldsymbol{\Delta}_1) \\ &= \frac{d\boldsymbol{R}(\boldsymbol{x}_1)}{dt}\boldsymbol{x}_2 + \boldsymbol{R}(\boldsymbol{x}_1)\dot{\boldsymbol{x}}_2 + \dot{\boldsymbol{\Delta}}_1 \end{aligned} \tag{13}$$

Differentiate $\boldsymbol{R}(\boldsymbol{x}_1)$, one obtains

$$\frac{d\boldsymbol{R}(\boldsymbol{x}_1)}{dt} = \begin{bmatrix} \sin\alpha\tan\beta\dot{\alpha} - \cos\alpha\sec^2\beta\dot{\beta} & 0 & -\cos\alpha\tan\beta\dot{\alpha} - \sin\alpha\sec^2\beta\dot{\beta} \\ \cos\alpha\dot{\alpha} & 0 & \sin\alpha\dot{\alpha} \\ \sin\alpha\cos\beta\dot{\alpha} - \cos\alpha\tan\beta\sec\beta\dot{\beta} & 0 & -\cos\alpha\cos\beta\dot{\alpha} - \cos\alpha\tan\beta\sec\beta\dot{\beta} \end{bmatrix} \tag{14}$$

Substituting (8) and (14) into (13) yields

$$\begin{aligned} \ddot{\boldsymbol{x}}_1 = &\frac{d\boldsymbol{R}(\boldsymbol{x}_1)}{dt}\boldsymbol{x}_2 - \boldsymbol{R}(\boldsymbol{x}_1)\boldsymbol{I}_n^{-1}\boldsymbol{x}_2^{\times}\boldsymbol{I}_n\boldsymbol{x}_2 \\ &\times \boldsymbol{R}(\boldsymbol{x}_1)\boldsymbol{I}_n^{-1}(-\boldsymbol{x}_2^{\times}\Delta\boldsymbol{I}\boldsymbol{x}_2 - \Delta\boldsymbol{I}\dot{\boldsymbol{x}}_2) \\ &+ \boldsymbol{R}(\boldsymbol{x}_1)\boldsymbol{I}_n^{-1}\boldsymbol{u} + \boldsymbol{R}(\boldsymbol{x}_1)\boldsymbol{I}_n^{-1}\boldsymbol{\Delta}_2 + \dot{\boldsymbol{\Delta}}_1 \end{aligned} \tag{15}$$

By the following definition

$$\begin{aligned} \boldsymbol{F}_0 &\triangleq \frac{d\boldsymbol{R}(\boldsymbol{x}_1)}{dt}\boldsymbol{x}_2 - \boldsymbol{R}(\boldsymbol{x}_1)\boldsymbol{I}_n^{-1}\boldsymbol{x}_2^{\times}\boldsymbol{I}_n\boldsymbol{x}_2, \\ y\Delta\boldsymbol{F} &\triangleq \boldsymbol{R}(\boldsymbol{x}_1)\boldsymbol{I}_n^{-1}(-\boldsymbol{x}_2^{\times}\Delta\boldsymbol{I}\boldsymbol{x}_2 - \Delta\boldsymbol{I}\dot{\boldsymbol{x}}_2), \\ \boldsymbol{G}_0 &\triangleq \boldsymbol{R}(\boldsymbol{x}_1)\boldsymbol{I}_n^{-1}, \\ \boldsymbol{\Delta}_3 &\triangleq \boldsymbol{R}(\boldsymbol{x}_1)\boldsymbol{I}_n^{-1}\boldsymbol{\Delta}_2 + \dot{\boldsymbol{\Delta}}_1, \end{aligned}$$

one can obtain

$$\ddot{\boldsymbol{x}}_1 = \boldsymbol{F}_0 + \boldsymbol{G}_0\boldsymbol{u} + \boldsymbol{F}_d \tag{16}$$

where $\boldsymbol{F}_d = \Delta\boldsymbol{F} + \boldsymbol{\Delta}_3$. Substituting (9) into (16) yields

$$\ddot{\boldsymbol{x}}_1 = \boldsymbol{F}_0 + \boldsymbol{G}_0(\boldsymbol{\Theta}\boldsymbol{u}_d + \boldsymbol{\rho}) + \boldsymbol{F}_d \tag{17}$$

Combined with (12), (17) can be expressed as

$$\begin{cases} \dot{z}_1 = z_2 \\ \dot{z}_2 = \boldsymbol{F}_0 + \boldsymbol{G}_0(\boldsymbol{\Theta}\boldsymbol{u}_d + \boldsymbol{\rho}) + \boldsymbol{F}_d - \ddot{\boldsymbol{x}}_{1d} \end{cases} \tag{18}$$

Assumption 1 ([5], [41]): $\boldsymbol{F}_0$, $\boldsymbol{G}_0$, $\boldsymbol{F}_d$, z_1, z_2, $\ddot{\boldsymbol{x}}_{1d}$ are bounded and the following inequalities exist

$$\|\boldsymbol{F}_0\| \leq \xi_0 \|\boldsymbol{x}_2\|^2 \tag{19}$$

$$\underline{g} < \|\boldsymbol{G}_0\| < \bar{g} \tag{20}$$

$$\|\boldsymbol{F}_d\| < \xi_1 + \xi_2 \|\boldsymbol{x}_2\|^2 \tag{21}$$

$$\|z_1\| < \xi_{z1}, \quad \|z_2\| < \xi_{z2}, \ \|\ddot{\boldsymbol{x}}_{1d}\| < \xi_{2d} \tag{22}$$

where ξ, ξ_1, ξ_2, $\underline{g}$, $\bar{g}$, ξ_{z1}, ξ_{z2} and ξ_{2d} are positive constants.

Therefore, the control objective can be formulated as

$$\lim_{t \to t_1} \|z_1\| = \lim_{t \to t_1} \|\boldsymbol{e}\| = 0 \tag{23}$$

where $t_1 \in (0, +\infty)$. When (23) holds, the aerodynamic angels α, β, μ can track the desired angels α_d, β_d, μ_d.

III. IMPROVED ADAPTIVE INTEGRAL SLIDING MODE FAULT-TOLERANT CONTROL LAW

In order to accomplish the fault-tolerant control law design mentioned above, a new improved integral sliding mode controller is proposed at the very beginning. Then combined with the improved integral sliding mode controller, an adaptive fault-tolerant control law is designed, as a result, the tracking error will converge with fast transient process even in the present of unknown uncertainties and actuator failure.

A. IMPROVED INTEGRAL SLIDING MODE CONTROL LAW DESIGN

In this section, an improved integral sliding mode control law is proposed for double integral system (1), aiming at obtaining quicker convergence. Firstly, an integral sliding mode manifold s is given as follows

$$s = o_2 + \int_0^t k_1 sig^{a_1}(o_1) ds + \int_0^t k_2 sig^{a_2}(o_2) ds \tag{24}$$

where $a_1 = \frac{a_2 a_3}{2a_3 - a_2}$, $a_2 \in (0, 1)$, $a_3 = 1$. Then, motivated by [38] and [39], an improved integral sliding control law is designed for double integral system (1) as follows

$$v_n = -R^{-1}\boldsymbol{B}^T \boldsymbol{P} \boldsymbol{sig} \tag{25}$$

where

$$\boldsymbol{sig} = \begin{cases} [sig^{a_1}(o_1), sig^{a_2}(o_2)]^T, & |o_j| \leq a_j^{1/(1-a_j)} (j = 1, 2) \\ \boldsymbol{o}, & \text{otherwise} \end{cases} \tag{26}$$

where $\boldsymbol{o} = [o_1, o_2]^T$, $\boldsymbol{B} = [0, 1]^T$, $\boldsymbol{a} = [a_1, a_2]^T$. R is a positive constant and obeys the following linear-quadratic performance index

$$J = \int_0^\infty (\boldsymbol{o}^T \boldsymbol{Q} \boldsymbol{o} + R v_n^2) dt. \tag{27}$$

$\boldsymbol{P}$ is the positive-define solution of the algebraic matrix Riccati equation

$$\boldsymbol{P}\boldsymbol{A} + \boldsymbol{A}^T \boldsymbol{P} + \boldsymbol{Q} - \boldsymbol{P}\boldsymbol{B}R^{-1}\boldsymbol{B}^T \boldsymbol{P} = 0 \tag{28}$$

where $\boldsymbol{A} = \begin{bmatrix} 0 & 1 \\ 0 & 0 \end{bmatrix}$. Thus $\boldsymbol{K} = [k_1, k_2]^T = R^{-1}\boldsymbol{B}^T \boldsymbol{P}$.

With the help of control law (25), the closed-loop system (1) will be stable in finite time. Then the following theorem can be obtained.

Theorem 1: The system states o_1, o_2 in (1) will converge to origin in finite time under the control law (25) with $a_3 = 1$, $a_2 \in (0, 1)$ and $a_1 = \frac{a_2 a_3}{2a_3 - a_2}$.

Proof: There are two cases to be discussed.

Case 1: $|o_i| > a_j^{1/(1-a_j)}$

If $|o_i| > a_j^{1/(1-a_j)}$, the control law v_n in (25) becomes

$$v_{n1} = -R^{-1}\boldsymbol{B}^T \boldsymbol{P} \boldsymbol{o}. \tag{29}$$

Obviously, (1) can be written in the form of state space as follows

$$\dot{\boldsymbol{o}} = \boldsymbol{A}\boldsymbol{o} + \boldsymbol{B}v_{n1}. \tag{30}$$

where A is the state matrix of (30), and B is the control input matrix of (30). Therefore v_{n1} acts as the optimal control law for double integral system (1) [38]. Therefore the system states of (1) will converge to a region $\boldsymbol{O} = \left\{(o_1, o_2) : |o_j| < a_j^{1/(1-a_j)} (j = 1, 2)\right\}$.

Case 2: $|o_i| \leq a_j^{1/(1-a_j)}$

If $|o_i| \leq a_j^{1/(1-a_j)}$, the control law v_n in (25) becomes

$$v_{n2} = -R^{-1}\boldsymbol{B}^T \boldsymbol{P} \boldsymbol{sig}^{\boldsymbol{a}}(\boldsymbol{o}). \tag{31}$$

According to optimal control theory, the elements in $R^{-1}\boldsymbol{B}^T \boldsymbol{P}$ are always positive. In fact, (31) is in accordance with (2). Then according to Lemma 1, when system states $o_1 \in \boldsymbol{O}$ and $o_2 \in \boldsymbol{O}$, the closed-loop system (1) will be stable in finite time.

Remark 1: Different from the existing methods designed in [38], we proposed a new strategy to improve the convergence speed of system states o_1, o_2. In [38], ''far from'' and ''near to'' are chosen as a condition to improve the convergence speed. However, it is not rigorous enough. Therefore we propose a strict condition to obtain fast convergence speed. For further analysis, define w_1 and w_2 as follows

$$w_1 = sig^{a_1}(o_1) \tag{32}$$

$$w_2 = o_1 \tag{33}$$

The graphical presentation of w_1 and w_2 *w.r.t.* o_1 in first quadrant is shown in Fig.1. Suppose that the parallel line w_{p2} of w_2 intersect w_1 at point C. Then we have the location of point C as $\left(a_1^{1/(1-a_1)}, a_1^{a_1/(1-a_1)}\right)$. It is clearly that, system state o_1 converges to origin on w_2 faster than that on w_1 inside Circle 1(see Fig1). Also, system state o_1 converges to origin on w_1 slower than that on w_2 outside Circle 1. Therefore, in control law (25), $a_1^{1/(1-a_1)}$ is chosen as the switching condition to design an improved control law.

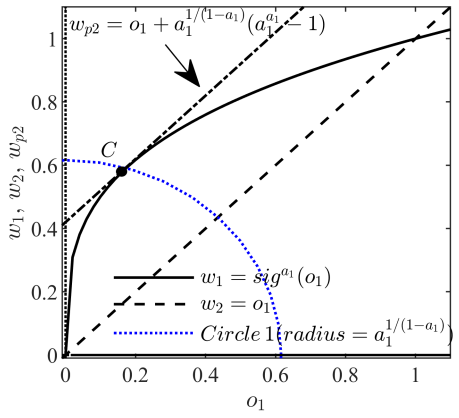

FIGURE 1. Graphical presentation of w_1, w_2, w_{p2}.

B. ADAPTIVE FAULT-TOLERANT CONTROL LAW BASED ON IMPROVED INTEGRAL SLIDING MODE

In this section, an adaptive fault-tolerant control law is developed based on integral sliding mode technology. With the help of the proposed control law, both the reachability of sliding surface and convergence of the system states in (18) can be guaranteed even in spite of unknown uncertainties, disturbance and actuator failure.

Firstly, based on Theorem 1, an integral sliding mode function vector $\boldsymbol{S}$ is as follows

$$\boldsymbol{S} = z_2 + \int_0^t \boldsymbol{c}_{z1} sig^{\boldsymbol{b}_{z1}}(z_1(s))ds + \int_0^t \boldsymbol{c}_{z2} sig^{\boldsymbol{b}_{z2}}(z_2(s))ds \tag{34}$$

where $\boldsymbol{S} = [s_1, s_2, s_3]^T$. $\boldsymbol{c}_{z1} = \text{diag}(c_1, c_1, c_1)$, $\boldsymbol{c}_{z2} = \text{diag}(c_2, c_2, c_2)$. $\boldsymbol{b}_{z1} = [b_1, b_1, b_1]^T$, $\boldsymbol{b}_{z2} = [b_2, b_2, b_2]^T$. The auxiliary equivalent control law $v_N = [v_{N1}, v_{N2}, v_{N3}]^T$. $v_{Ni}(i = 1, 2, 3)$ is designed in accordance with (25) in Theorem 1.

$$v_{Ni} = \begin{cases} -R^{-1}\boldsymbol{B}^T\boldsymbol{P}\boldsymbol{Sig}_i, & |z_{ij}| \le b_j^{1/(1-b_j)}(j = 1, 2) \\ -R^{-1}\boldsymbol{B}^T\boldsymbol{P}\boldsymbol{Z}_i, & \text{otherwise} \end{cases} \quad (i = 1, 2, 3) \tag{35}$$

where $\boldsymbol{Z}_i = [z_{1i}, z_{2i}]^T(i = 1, 2, 3)$ and $\boldsymbol{Sig}_i = [sig^{b_1}(z_{1i}(t)), sig^{b_2}(z_{2i}(t))]^T(i = 1, 2, 3)$.

Combining with integral sliding mode function (34), an adaptive sliding mode control law is proposed as follows

$$\boldsymbol{u}_d = \boldsymbol{u}_{eq} + \boldsymbol{u}_r + \boldsymbol{u}_c \tag{36}$$

where $\boldsymbol{u}_{eq} \in \mathcal{R}^{3\times1}$ is equivalent control law. $\boldsymbol{u}_r \in \mathcal{R}^{3\times1}$ forces the sliding function (34) converge. $\boldsymbol{u}_c \in \mathcal{R}^{3\times1}$ deals with the model uncertainty, external disturbances, and actuator failures. $\boldsymbol{u}_{eq}$ and $\boldsymbol{u}_r$ are given as follows

$$\boldsymbol{u}_{eq} = -\boldsymbol{G}_0^{-1}(\boldsymbol{F}_0 - \boldsymbol{v}_N - \ddot{\boldsymbol{x}}_{1d}) \tag{37}$$

$$\boldsymbol{u}_r = -\boldsymbol{G}_0^{-1}(\boldsymbol{\tau}\boldsymbol{s} + \boldsymbol{\eta}\text{sgn}(\boldsymbol{s})|\boldsymbol{s}|^{\frac{1}{2}}) \tag{38}$$

where $\boldsymbol{\tau} = \text{diag}(\tau_1, \tau_2, \tau_3), \tau_i > 0(i = 1, 2, 3)$. $\boldsymbol{\eta} = \text{diag}(\eta_1, \eta_2, \eta_3), \eta_i > 0(i = 1, 2, 3)$. Taking the time derivative of (34) yields

$$\dot{\boldsymbol{S}} = \dot{z}_2 + \boldsymbol{v}_N = \boldsymbol{F}_n + \boldsymbol{G}_0\boldsymbol{\Theta}\boldsymbol{u}_d + \boldsymbol{F}_d + \boldsymbol{F}_a \tag{39}$$

and

$$\boldsymbol{F}_a = \boldsymbol{G}_0\boldsymbol{\rho} \tag{40}$$

$$\boldsymbol{F}_n = \boldsymbol{F}_0 - \boldsymbol{v}_N - \ddot{\boldsymbol{x}}_{1d} \tag{41}$$

Substituting (36) and (37) into (39), it can be obtained

$$\dot{\boldsymbol{S}} = \boldsymbol{F}_N + \boldsymbol{G}_0\boldsymbol{\Theta}(\boldsymbol{u}_r + \boldsymbol{u}_c) + \boldsymbol{F}_d + \boldsymbol{F}_a \tag{42}$$

and

$$\boldsymbol{F}_N = (\boldsymbol{E} - \boldsymbol{G}_0\boldsymbol{\Theta}\boldsymbol{G}_0^{-1})\boldsymbol{F}_n \tag{43}$$

where $\boldsymbol{E} = \text{diag}(1, 1, 1)$.

Assumption 2 ([5]): Considering that $\boldsymbol{G}_0$ and $\boldsymbol{\rho}$ are bounded, it is obtained

$$\|\boldsymbol{F}_a\| \le g_b\rho_b \tag{44}$$

with $g_b = max\{|\underline{g}|, |\bar{g}|\}$, $\rho_b = max\{|\underline{\rho}|, |\bar{\rho}|\}$.

Assumption 3: Considering that $\bar{\boldsymbol{G}}_0$ and $\boldsymbol{\Theta}$ are bounded, there exists a positive constant ξ_3 such that

$$\|\boldsymbol{E} - \boldsymbol{G}_0\boldsymbol{\Theta}\boldsymbol{G}_0^{-1}\| \le \xi_3 \tag{45}$$

Then $\boldsymbol{u}_c$ can be obtained by

$$\boldsymbol{u}_c = \begin{cases} -\Phi\boldsymbol{G}_0\frac{\boldsymbol{s}}{\|\boldsymbol{s}\|}, & \Phi > \delta \\ -\Phi^2\boldsymbol{G}_0\frac{\boldsymbol{s}}{\delta}, & \Phi \le \delta \end{cases} \tag{46}$$

with δ is a boundary constant. $\Phi = \hat{\xi}_4\xi_5 + \hat{\xi}_6\xi_7 + \hat{\xi}_8$, $\hat{\xi}_4$, $\hat{\xi}_6$, $\hat{\xi}_8$ are the estimates of ξ_4, ξ_6, ξ_8 respectively and obey the following updating laws

$$\begin{cases} \dot{\hat{\xi}}_4 = -c_{41}\hat{\xi}_4 + c_{42}\xi_5\|\boldsymbol{s}\| \\ \dot{\hat{\xi}}_6 = -c_{61}\hat{\xi}_6 + c_{62}\xi_7\|\boldsymbol{s}\| \\ \dot{\hat{\xi}}_8 = -c_{81}\hat{\xi}_8 + c_{82}\|\boldsymbol{s}\| \end{cases} \tag{47}$$

and $\xi_4 = max\left\{\begin{matrix}(\xi_0\xi_{1d}^2 + \xi_{2d})\xi_3,\ \xi_0\xi_3,\ 2\xi_0\xi_{1d}\xi_3, \\ \lambda_{max}(\boldsymbol{c}_1)\sqrt{3}^{(1-b_1)}\|z_1\|^{b_1}\xi_3, \\ \lambda_{max}(\boldsymbol{c}_2)\sqrt{3}^{(1-b_2)}\|z_2\|^{b_2}\xi_3\end{matrix}\right\}$,

$\xi_5 = 1 + \|z_1\|^{b_1} + \|z_2\| + \|z_2\|^2 + \|z_2\|^{b_2}$,

$\xi_6 = max\left\{\xi_1 + \xi_2\xi_{1d}^2,\ 2\xi_2\xi,\ \xi_2\right\}$, $\xi_7 = 1 + \|z_2\| + \|z_2\|^2$,

$\xi_8 = g_b\rho_b$. c_{41}, c_{42}, c_{61}, c_{62} and c_{81}, c_{82} are designed positive constants.

Remark 2: According to Lemma 2, the following inequalities exist.

$$\|\boldsymbol{c}_{z1}sig^{\boldsymbol{b}_{z1}}(z_1(t))\| \le \lambda_{max}(\boldsymbol{c}_{z1})\sqrt{3}^{(1-b_1)}\|z_1\|^{b_1} \tag{48}$$

$$\|\boldsymbol{c}_{z2}sig^{\boldsymbol{b}_{z2}}(z_2(t))\| \le \lambda_{max}(\boldsymbol{c}_{z2})\sqrt{3}^{(1-b_2)}\|z_2\|^{b_2} \tag{49}$$

Hence the main result is given in the following theorem.

Theorem 2: For nonlinear system (18), the state variable $z_{ji}(i = 1, 2, 3, j = 1, 2)$ can converge to a neighborhood region of zero by defining a sliding function (34) and the adaptive fault-tolerant control law (36).

Proof: Select the Lyapunov functional candidate as

$$V = \frac{\boldsymbol{s}^T\boldsymbol{s}}{2} + \frac{\tilde{\xi}_4^2}{2c_{42}\lambda_2} + \frac{\tilde{\xi}_6^2}{2c_{62}\lambda_2} + \frac{\tilde{\xi}_8^2}{2c_{82}\lambda_2} \tag{50}$$

where $\tilde{\xi}_4 = \xi_4 - \lambda_2\hat{\xi}_4$, $\tilde{\xi}_6 = \xi_6 - \lambda_2\hat{\xi}_6$, $\tilde{\xi}_8 = \xi_8 - \lambda_2\hat{\xi}_8$ and $\lambda_2 = \lambda_{min}(\boldsymbol{G}_0\boldsymbol{\Theta}\boldsymbol{G}_0)$. Taking the time derivate of (50) and using (36)-(38) and (42) yield

$$\begin{aligned}\dot{V} &= \boldsymbol{s}^T\boldsymbol{G}_0\boldsymbol{\Theta}\boldsymbol{u}_r + \boldsymbol{s}^T(\boldsymbol{F}_N + \boldsymbol{F}_d + \boldsymbol{F}_a) \\ &\quad + \boldsymbol{s}^T\boldsymbol{G}_0\boldsymbol{\Theta}\boldsymbol{u}_c + \frac{c_{41}}{c_{42}}\tilde{\xi}_4\hat{\xi}_4 - \tilde{\xi}_4\xi_5\|\boldsymbol{s}\| \\ &\quad + \frac{c_{61}}{c_{62}}\tilde{\xi}_6\hat{\xi}_6 - \tilde{\xi}_6\xi_7\|\boldsymbol{s}\| + \frac{c_{81}}{c_{82}}\tilde{\xi}_8\hat{\xi}_8 - \tilde{\xi}_8\|\boldsymbol{s}\| \end{aligned} \tag{51}$$

Obviously, the following inequalities can be obtained.

$$\begin{aligned}\boldsymbol{s}^T(\boldsymbol{F}_N + \boldsymbol{F}_d + \boldsymbol{F}_a) &\le \|\boldsymbol{s}\|(\|\boldsymbol{F}_N\| + \|\boldsymbol{F}_d\| + \|\boldsymbol{F}_a\|) \\ &\le (\xi_4\xi_5 + \xi_6\xi_7 + \xi_8)\|\boldsymbol{s}\| \end{aligned},$$

$$\begin{aligned}\boldsymbol{s}^T\boldsymbol{G}_0\boldsymbol{\Theta}\boldsymbol{u}_r &= -\boldsymbol{G}_0\boldsymbol{\Theta}\boldsymbol{G}_0^{-1}\tau\|\boldsymbol{s}\|^2 - \boldsymbol{G}_0\boldsymbol{\Theta}\boldsymbol{G}_0^{-1}\eta\|\boldsymbol{s}\|^{\frac{3}{2}} \\ &\le -\lambda_1\tau\|\boldsymbol{s}\|^2 - \lambda_1\eta\|\boldsymbol{s}\|^{\frac{3}{2}} \end{aligned}.$$

where $\lambda_1 = \lambda_{min}(\boldsymbol{G}_0\boldsymbol{\Theta}\boldsymbol{G}_0^{-1})$. Then, (51) turns to

$$\begin{aligned}\dot{V} &\le -\lambda_1\tau\|\boldsymbol{s}\|^2 - \lambda_1\eta\|\boldsymbol{s}\|^{\frac{3}{2}} \\ &\quad + \lambda_2\hat{\xi}_4\xi_5\|\boldsymbol{s}\| + \lambda_2\hat{\xi}_6\xi_7\|\boldsymbol{s}\| + \lambda_2\hat{\xi}_8\|\boldsymbol{s}\| \\ &\quad + \frac{c_{41}}{c_{42}}\tilde{\xi}_4\hat{\xi}_4 + \frac{c_{61}}{c_{62}}\tilde{\xi}_6\hat{\xi}_6 + \frac{c_{81}}{c_{82}}\tilde{\xi}_8\hat{\xi}_8 + \boldsymbol{s}^T\boldsymbol{G}_0\boldsymbol{\Theta}\boldsymbol{u}_c \\ &\le -\lambda_1\tau\|\boldsymbol{s}\|^2 - \frac{c_{41}\tilde{\xi}_4^2}{2\lambda_2 c_{42}} - \frac{c_{61}\tilde{\xi}_6^2}{2\lambda_2 c_{62}} - \frac{c_{81}\tilde{\xi}_8^2}{2\lambda_2 c_{82}} \\ &\quad - \lambda_1\eta\|\boldsymbol{s}\|^{\frac{3}{2}} + \lambda_2\hat{\xi}_4\xi_5\|\boldsymbol{s}\| + \lambda_2\hat{\xi}_6\xi_7\|\boldsymbol{s}\| + \lambda_2\hat{\xi}_8\|\boldsymbol{s}\| \\ &\quad + \boldsymbol{s}^T\boldsymbol{G}_0\boldsymbol{\Theta}\boldsymbol{u}_c + \frac{c_{41}\xi_4^2}{2\lambda_2 c_{42}} + \frac{c_{61}\xi_6^2}{2\lambda_2 c_{62}} + \frac{c_{81}\xi_8^2}{2\lambda_2 c_{82}} \end{aligned} \tag{52}$$

Combined with (50), it can be obtained

$$\begin{aligned}\dot{V} &\le -\tau_1 V - \lambda_1\eta\|\boldsymbol{s}\|^{\frac{3}{2}} + \tau_2 + \boldsymbol{s}^T\boldsymbol{G}_0\boldsymbol{\Theta}\boldsymbol{u}_c \\ &\quad + \lambda_2\hat{\xi}_4\xi_5\|\boldsymbol{s}\| + \lambda_2\hat{\xi}_6\xi_7\|\boldsymbol{s}\| + \lambda_2\hat{\xi}_8\|\boldsymbol{s}\| \end{aligned} \tag{53}$$

where $-\tau\lambda_1\|s\|^2 - \eta\lambda_1\|s\|^{\frac{3}{2}}$, $\tau_2 = \frac{c_{41}}{2\lambda_2\ c_{42}}\xi_4^2 + \frac{c_{61}}{2\lambda_2\ c_{62}}\xi_6^2 + \frac{c_{81}}{2\lambda_2\ c_{82}}\xi_8^2$.

Then there are two cases to be discussed.

Case 1: If $\Phi > \delta$, substituting the first equation in (46) into (51) yields

$$\begin{aligned}\dot{V} &\le -\tau_1 V - \lambda_1\eta\|\boldsymbol{s}\|^{\frac{3}{2}} + \tau_2 \\ &\quad + \lambda_2\hat{\xi}_4\xi_5\|\boldsymbol{s}\| + \lambda_2\hat{\xi}_6\xi_7\|\boldsymbol{s}\| + \lambda_2\hat{\xi}_8\|\boldsymbol{s}\| \\ &\quad - \Phi\lambda_2\|\boldsymbol{s}\| \end{aligned} \tag{54}$$

with $\lambda_2 = \lambda_{min}(\boldsymbol{G}_0\boldsymbol{\Theta}\boldsymbol{G}_0)$. Then one has

$$\begin{aligned}\dot{V} &\le -\tau_1 V - \lambda_1\eta\|\boldsymbol{s}\|^{\frac{3}{2}} + \tau_2 \\ &\quad + \lambda_2\hat{\xi}_4\xi_5\|\boldsymbol{s}\| + \lambda_2\hat{\xi}_6\xi_7\|\boldsymbol{s}\| + \lambda_2\hat{\xi}_8\|\boldsymbol{s}\| \\ &\quad - \lambda_2(\hat{\xi}_4\xi_5 + \hat{\xi}_6\xi_7 + \hat{\xi}_8)\|\boldsymbol{s}\| \\ &\le -\tau_1 V - \lambda_1\eta\|\boldsymbol{s}\|^{\frac{3}{2}} + \tau_2 \end{aligned} \tag{55}$$

Case 2: If $\Phi \le \delta$, substituting the second equation in (46) into (51) yields

$$\begin{aligned}\dot{V} &\le -\tau_1 V - \lambda_1\eta\|\boldsymbol{s}\|^{\frac{3}{2}} + \tau_2 - \lambda_2\Phi^2\frac{\|\boldsymbol{s}\|^2}{\delta} \\ &\quad \times \lambda_2\hat{\xi}_4\xi_5\|\boldsymbol{s}\| + \lambda_2\hat{\xi}_6\xi_7\|\boldsymbol{s}\| + \lambda_2\hat{\xi}_8\|\boldsymbol{s}\| \\ &\le -\tau_1 V - \lambda_1\eta\|\boldsymbol{s}\|^{\frac{3}{2}} + \tau_2 \\ &\quad + \lambda_2\Phi\|\boldsymbol{s}\| - \lambda_2\Phi^2\frac{\|\boldsymbol{s}\|^2}{\delta} \end{aligned} \tag{56}$$

Obviously, the maximum value of $\lambda_2\Phi\|\boldsymbol{s}\| - \lambda_2\Phi^2\frac{\|\boldsymbol{s}\|^2}{\delta}$ is $\tau_3 = \frac{1}{4}\lambda_2\delta$ when $\Phi\|\boldsymbol{s}\| = \frac{1}{2}\delta$. Then one has the following inequality

$$\dot{V} \le -\tau_1 V - \lambda_1\eta\|\boldsymbol{s}\|^{\frac{3}{2}} + \tau_2 + \tau_3 \tag{57}$$

Note that

$$\|\boldsymbol{s}\|^{1+\frac{1}{2}} = 2^{\frac{3}{4}}(\frac{1}{2}\boldsymbol{s}^T\boldsymbol{s})^{\frac{3}{4}} \ge (\frac{1}{2}\boldsymbol{s}^T\boldsymbol{s})^{\frac{3}{4}} \tag{58}$$

Then one has

$$-(\frac{1}{2}\boldsymbol{s}^T\boldsymbol{s})^{\frac{3}{4}} \le -V^{\frac{3}{4}} + \tau_4 \tag{59}$$

where $\tau_4 = (\frac{\tilde{\xi}_4^2}{2c_{42}\lambda_2})^{\frac{3}{4}} + (\frac{\tilde{\xi}_6^2}{2c_{62}\lambda_2})^{\frac{3}{4}} + (\frac{\tilde{\xi}_8^2}{2c_{82}\lambda_2})^{\frac{3}{4}}$.

Then (55) and (57) turns

$$\begin{cases}\dot{V} & \le -\tau_1 V - \lambda_1\eta V^{\frac{3}{4}} + \tau_2 \\ \dot{V} & \le -\tau_1 V - \lambda_1\eta V^{\frac{3}{4}} + \tau_5 \end{cases} \tag{60}$$

where $\tau_5 = \tau_2 + \tau_3 + \tau_4$.

Therefore, the sliding surface will be stabilized into the region Ω,

$$\Omega = \left\{\|s\| \le min\left\{\sqrt{\frac{2\tau_6}{\tau_1}},\ \sqrt{2}\left(\frac{\tau_6}{\lambda_1\eta}\right)^{\frac{2}{3}}\right\}\right\} \tag{61}$$

where $\tau_6 = max\{\tau_2,\ \tau_5\}$. Therefore, the sliding mode function will converge to the neighborhood of $\|\boldsymbol{s}\| = 0$, that is, the real sliding mode is established. Thus it can be obtained that

$$|\dot{s}_1| \le \tau_{s1}, \quad |\dot{s}_2| \le \tau_{s2},\ |\dot{s}_3| \le \tau_{s3} \tag{62}$$

where $\tau_{s1} > 0$, $\tau_{s2} > 0$, $\tau_{s3} > 0$.

Thus, we have

$$\dot{\boldsymbol{z}}_2(t) + \boldsymbol{c}_{z1}\boldsymbol{sig}^{\boldsymbol{b}_{z1}}(\boldsymbol{z}_1(\boldsymbol{s})) + \boldsymbol{c}_{z2}\boldsymbol{sig}^{\boldsymbol{b}_{z2}}(\boldsymbol{z}_2(\boldsymbol{s})) = \boldsymbol{\tau}_s \tag{63}$$

where $\boldsymbol{\tau}_s = [\tau_{s1},\ \tau_{s2},\ \tau_{s3}]^T$. By resorting to Theorem 1, $\boldsymbol{z}_{ji}(j = 1, 2, i = 1, 2, 3)$ will converge to a vicinity of the origin in finite time.

IV. SIMULATION

This section carries out several simulations to evaluate the improved integral sliding mode control law (25) and the proposed adaptive fault-tolerant control law (36) for HSV attitude control. Simulation experiment is carried out by MATLAB R2018b.

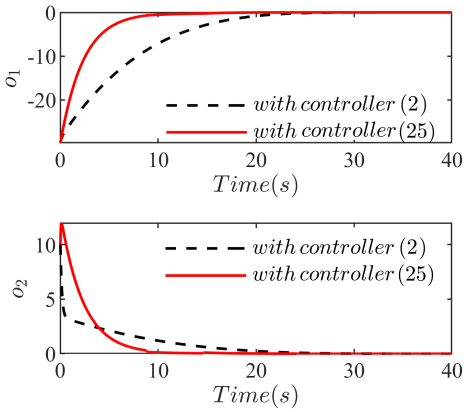

FIGURE 2. Comparison results of states o_1, o_2 under controller (21) and the controller (25).

A. NUMERICAL EXAMPLE 1

Consider the double integral system (1) and rewrite (1) as below

$$\begin{cases} \dot{o}_1 = o_2 \\ \dot{o}_2 = v \end{cases} \tag{64}$$

Controller (2) and controller (25) are used for double integral system (64) respectively. Initial values are set as $o_1(0) = -30$ and $o_2(0) = 10$. Parameters in controller (2) and controller (25) are set as $a_2 = 2/3$. $R = 35, \boldsymbol{Q} = \begin{bmatrix} 10 & 0 \\ 0 & 20 \end{bmatrix}$. $\boldsymbol{K} = R^{-1}\boldsymbol{B}^T\boldsymbol{P}$ and $\boldsymbol{P}$ is the positive-define solution of (28). As a result, (25) turns

$$v_n = \begin{cases} -\boldsymbol{K}\boldsymbol{o}, & |o_j| > (\frac{2}{3})^{\frac{1}{1-\frac{2}{3}}} \\ -\boldsymbol{K}\boldsymbol{sig}^{\boldsymbol{a}}(\boldsymbol{o}), & |o_j| \le (\frac{2}{3})^{\frac{1}{1-\frac{2}{3}}} \end{cases} \quad (j = 1, 2) \tag{65}$$

Simulation result is illustrated in Fig.2. It is clearly that the convergence speed of $o_j (j = 1, 2)$ with controller (25) is faster evidently than that with controller (2). Also, as is shown in Fig.3, with the improved controller (25), the establishment of sliding mode can be obtained faster than that with the controller (2).

B. NUMERICAL EXAMPLE 2

In this subsection, several simulation results are presented to evaluate the effectiveness of the proposed fault-tolerant controller (36). The mathematical model of HSV attitude control is given by (5). Initial system states are set as $\alpha(0) = 6deg$, $\beta(0) = 0\ deg$, $\mu(0) = 1\ deg$. $p(0) = 0deg/s$, $q(0) = 0deg/s$, $r(0) = 0deg/s$. The desired aerodynamic angel vector is set as $[\alpha_d, \beta_d, \mu_d]^T = [3deg, 0deg, 3deg]T$. The parameters in $v_{Ni} (i = 1, 2, 3)$ are set in accordance with (65). Other parameters used are listed in Table 1. The model parameters and aerodynamics coefficients used herein can be found in [45].

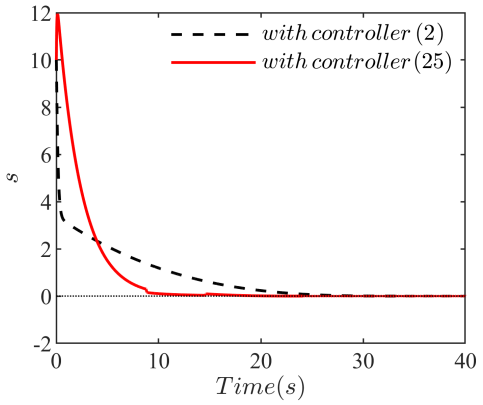

FIGURE 3. Sliding surface s.

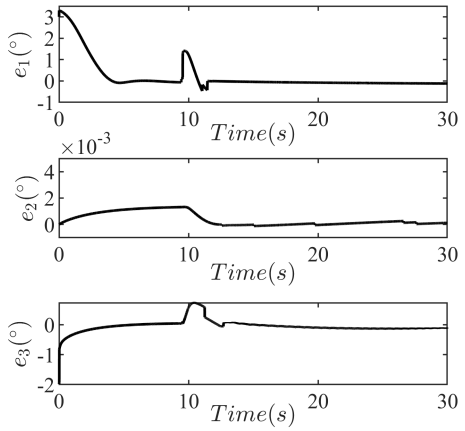

FIGURE 4. Tracking error of attitude angle.

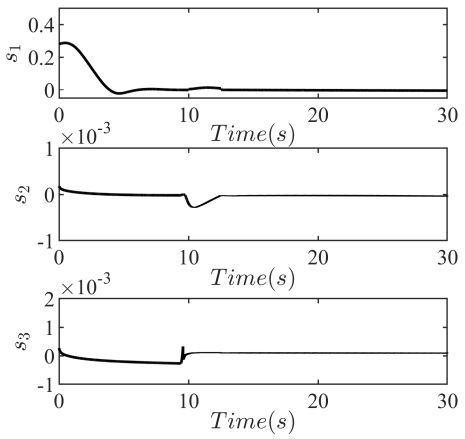

FIGURE 5. Sliding mode surface s_1, s_2, s_3.

The external disturbance is defined as $\Delta\boldsymbol{M}$ and is set as follows,

$$\Delta\boldsymbol{M} = \begin{bmatrix} 1 + \sin(\pi t/125) \\ 1 + \sin(\pi t/125) \\ 1 + \sin(\pi t/125) \end{bmatrix} \times 10^4 (N \cdot m).$$

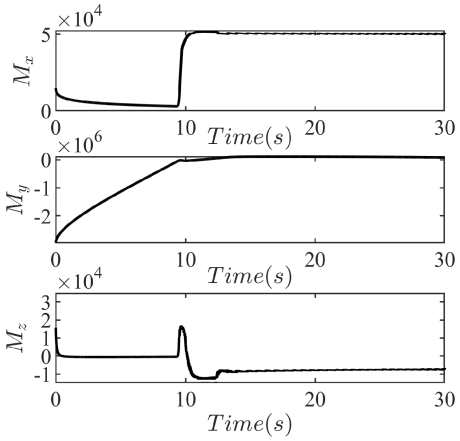

FIGURE 6. Control torque.

TABLE 1. Controller parameters.

Parameters	Value
$\boldsymbol{\tau}$	$\mathrm{diag}(9, 4, 14)$
c_{41}, c_{61}, c_{81}	$1.4, 1, 0.12$
$\boldsymbol{\eta}$	$\mathrm{diag}(1, 1, 1) \times 10^{-3}$
c_{42}, c_{62}, c_{82}	$2, 2.5, 2.5$
b_2	$2/3$
$\theta_i (i = 1, 2, 3)$	0.3
δ	0.01
$\rho_i (i = 1, 2, 3)$	$10^4 (N \cdot m)$

The environment uncertainties are set as $\Delta I = 10\% I$, 20% bias atmospheric density and 10% bias for aerodynamic coefficients. The actuator faults factor $\theta_i (i = 1, 2, 3)$ and $\rho_i (i = 1, 2, 3)$ are given in Table 1.

Assume that the actuators fail at $t = 9s$, it is clearly that the actuator failures have the adverse impact on the closed-loop system(See Fig.4-Fig.6). When actuator fails, the control inputs undergo very obvious changes(Fig.6). It leads to a noticeable fluctuation which occurs in the tracking error of attitude angle e_1, e_2, e_3(Fig.4) and sliding mode surface(Fig.5). Fortunately, with the help of the proposed fault-tolerant controller (36), the performance degradation of the faulty closed-system can be stopped soon. Clearly, within 5s, the attitude angle tracking error e_1, e_2 and e_3 return to the vicinity of origin(Fig.4). Meanwhile the establishment of sliding mode is achieved again(Fig.5). The control input torques are also readjusted(Fig.6).

V. CONCLUSION

For addressing the fault-tolerant control problem for the attitude system of HSV, an improved adaptive integral sliding mode fault-tolerant controller is presented. With the proposed fault-tolerant controller, the transient process of the system states will be accelerated. Meanwhile, the adaptive compensation part in the proposed fault-tolerant control provides the closed-loop system the assurance in stability even in the present of additive fault and multiplicative fault. Concurrently, the need for bound of unknown uncertainty and unknown fault is removed. The simulation example has shown the effectiveness of the proposed fault-tolerant control strategy. Furthermore, in our future work, other types of fault will be considered, such as sensor faults and system faults, and so forth.

REFERENCES

[1] J. W. Wang and R. Zhang, "Terminal guidance for a hypersonic vehicle with impact time control," *J. Guid., Control, Dyn.*, vol. 41, no. 8, pp. 1789–1797, Aug. 2018.
[2] Z. Hewei and L. Rui, "Typical adaptive neural control for hypersonic vehicle based on higher-order filters," *J. Syst. Eng. Electron.*, vol. 31, no. 5, pp. 1031–1040, Oct. 2020.
[3] Y. Guo, B. Xu, X. Hu, X. Bu, and Y. Zhang, "Two controller designs of hypersonic flight vehicle under actuator dynamics and AOA constraint," *Aerosp. Sci. Technol.*, vol. 80, pp. 11–19, Sep. 2018.
[4] Q. Zong, J. Wang, B. Tian, and Y. Tao, "Quasi-continuous high-order sliding mode controller and observer design for flexible hypersonic vehicle," *Aerosp. Sci. Technol.*, vol. 27, no. 1, pp. 127–137, Jun. 2013.
[5] Y.-Z. Sheng, J. Geng, X.-D. Liu, and L. Wang, "Nonsingular finite-time second order sliding mode attitude control for reentry vehicle," *Int. J. Control, Autom. Syst.*, vol. 13, no. 4, pp. 853–866, May 2015.
[6] M. Sagliano, E. Mooij, and S. Theil, "Adaptive disturbance-based high-order sliding-mode control for hypersonic-entry vehicles," *J. Guid., Control, Dyn.*, vol. 40, no. 3, pp. 521–536, Mar. 2017.
[7] Q. Mao, L. Dou, Q. Zong, and Z. Ding, "Attitude control design for reusable launch vehicles using adaptive fuzzy control with compensation controller," *Proc. Inst. Mech. Eng., G, J. Aerosp. Eng.*, vol. 233, no. 3, pp. 823–836, Nov. 2017.
[8] Y. Z. Meng, B. Jiang, and R. Y. Qi, "Adaptive fault-tolerant attitude tracking control of hypersonic vehicle subject to unexpected centroid-shift and state constraints," *Aerosp. Sci. Technol.*, vol. 95, pp. 1–13, Dec. 2019.
[9] J. Zhao, B. Jiang, P. Shi, and H. Liu, "Adaptive dynamic sliding mode control for near space vehicles under actuator faults," *Circuits, Syst., Signal Process.*, vol. 32, no. 5, pp. 2281–2296, Mar. 2013.
[10] X.-N. Shi, Y.-A. Zhang, D. Zhou, and Z.-G. Zhou, "Global fixed-time attitude tracking control for the rigid spacecraft with actuator saturation and faults," *Acta Astronautica*, vol. 155, pp. 325–333, Feb. 2019.
[11] Y. Yu, H. Wang, and N. Li, "Fault-tolerant control for over-actuated hypersonic reentry vehicle subject to multiple disturbances and actuator faults," *Aerosp. Sci. Technol.*, vol. 87, pp. 230–243, Apr. 2019.
[12] H. An, C. Wang, and B. Fidan, "Sliding mode disturbance observer-enhanced adaptive control for the air-breathing hypersonic flight vehicle," *Acta Astronautica*, vol. 139, pp. 111–121, Oct. 2017.
[13] P. Lu, E. van Kampen, C. C. de Visser, and Q. P. Chu, "Framework for simultaneous sensor and actuator fault-tolerant flight control," *J. Guid., Control, Dyn.*, vol. 40, no. 8, pp. 2127–2135, Aug. 2017.
[14] M. Sami and R. J. Patton, "Active fault tolerant control for nonlinear systems with simultaneous actuator and sensor faults," *Int. J. Control, Autom. Syst.*, vol. 11, no. 6, pp. 1149–1161, Nov. 2013.
[15] Z.-F. Gao, J.-X. Lin, and T. Cao, "Robust fault tolerant tracking control design for a linearized hypersonic vehicle with sensor fault," *Int. J. Control, Autom. Syst.*, vol. 13, no. 3, pp. 672–679, Mar. 2015.
[16] M.-Z. Gao, G.-P. Cai, and Y. Nan, "Robust adaptive fault-tolerant H_∞ control of reentry vehicle considering actuator and sensor faults based on trajectory optimization," *Int. J. Control, Autom. Syst.*, vol. 14, no. 1, pp. 198–210, Feb. 2016.
[17] Y. Zhang and J. Jiang, "Bibliographical review on reconfigurable fault-tolerant control systems," *Annu. Rev. Control*, vol. 32, no. 2, pp. 229–252, Dec. 2008.
[18] Y. Xu, B. Jiang, Z. Gao, and K. Zhang, "Fault tolerant control for near space vehicle: A survey and some new results," *J. Syst. Eng. Electron.*, vol. 22, no. 1, pp. 88–94, Feb. 2011.
[19] Z. Wang, W. Bao, and H. Li, "Second-order dynamic sliding-mode control for nonminimum phase underactuated hypersonic vehicles," *IEEE Trans. Ind. Electron.*, vol. 64, no. 4, pp. 3105–3112, Apr. 2017.
[20] A. Emami and A. Banazadeh, "Fault-tolerant predictive trajectory tracking of an air vehicle based on acceleration control," *IET Control Theory Appl.*, vol. 14, no. 5, pp. 1–14, Dec. 2019.
[21] J. Zhao, B. Jiang, X. Fei, Z. F. Gao, and Y. F. Xu, "Adaptive sliding mode backstepping control for near space vehicles considering engine faults," *J. Syst. Eng. Electron.*, vol. 29, no. 2, pp. 343–351, Apr. 2018.

[22] F. H. Guo, X. D. Liu, and X. S. Li, "Fault-tolerant controller based on integral sliding mode with prescribed performance for hypersonic re-entry vehicle," in *Proc. Chin. Control Conf. (CCC)*, Guangzhou, China, 2019, pp. 5012–5017.
[23] B. Jiang, D. Xu, P. Shi, and C. C. Lim, "Adaptive neural observer-based backstepping fault tolerant control for near space vehicle under control effector damage," *IET Control Theory Appl.*, vol. 8, no. 9, pp. 658–666, Jun. 2014.
[24] R. Qi, Y. Huang, B. Jiang, and G. Tao, "Adaptive backstepping control for a hypersonic vehicle with uncertain parameters and actuator faults," *Proc. Inst. Mech. Eng., I, J. Syst. Control Eng.*, vol. 227, no. 1, pp. 51–61, Jan. 2013.
[25] X. Hu, H. R. Karimi, L. Wu, and Y. Guo, "Model predictive control-based non-linear fault tolerant control for air-breathing hypersonic vehicles," *IET Control Theory Appl.*, vol. 8, no. 13, pp. 1147–1153, Sep. 2014.
[26] C. Hu, X. Wei, L. Cao, Y. Tao, Z. Gao, and Y. Hu, "Integrated fault-tolerant control system design based on continuous model predictive control for longitudinal manoeuvre of hypersonic vehicle with actuator faults," *IET Control Theory Appl.*, vol. 14, no. 13, pp. 1769–1784, Jul. 2020.
[27] C. Ming, R. Sun, and B. Zhu, "Nonlinear fault-tolerant control with prescribed performance for air-breathing supersonic missiles," *J. Spacecraft Rockets*, vol. 54, no. 5, pp. 1092–1099, Sep. 2017.
[28] R. Y. Zhai, R. Y. Qi, and B. Jiang, "Adaptive sliding mode fault-tolerant control for hypersonic vehicle based on radial basis function neural networks," *Int. J. Adv. Robot Syst.*, vol. 14, no. 3, pp. 1–11, May 2017.
[29] Y. Sun, J. Xu, G. Lin, W. Ji, and L. Wang, "RBF neural network-based supervisor control for maglev vehicles on an elastic track with network time-delay," *IEEE Trans. Ind. Informat.*, early access, Oct. 19, 2020, doi: 10.1109/TII.2020.3032235.
[30] Y. Sun, J. Xu, H. Wu, G. Lin, and S. Mumtaz, "Deep learning based semi-supervised control for vertical security of maglev vehicle with guaranteed bounded airgap," *IEEE Trans. Intell. Transp. Syst.*, early access, Jan. 1, 2021, doi: 10.1109/TITS.2020.3045319.
[31] H. Sun, S. Li, and C. Sun, "Finite time integral sliding mode control of hypersonic vehicles," *Nonlinear Dyn.*, vol. 73, nos. 1–2, pp. 229–244, Jan. 2013.
[32] H. Sun, S. Li, and C. Sun, "Robust adaptive integral-sliding-mode fault-tolerant control for airbreathing hypersonic vehicles," *Proc. Inst. Mech. Eng., I, J. Syst. Control Eng.*, vol. 226, no. 10, pp. 1344–1355, Nov. 2012.
[33] Y. Ding, X. Wang, Y. Bai, and N. Cui, "Global smooth sliding mode controller for flexible air-breathing hypersonic vehicle with actuator faults," *Aerosp. Sci. Technol.*, vol. 92, pp. 563–578, Sep. 2019.
[34] J.-G. Sun, S.-M. Song, and G.-Q. Wu, "Fault-tolerant track control of hypersonic vehicle based on fast terminal sliding mode," *J. Spacecraft Rockets*, vol. 54, no. 6, pp. 1304–1316, Nov. 2017.
[35] X. Liang, Q. Wang, C. Hu, and C. Dong, "Fixed-time observer based fault tolerant attitude control for reusable launch vehicle with actuator faults," *Aerosp. Sci. Technol.*, vol. 107, Dec. 2020, Art. no. 106314.
[36] Q. Zong, J. Zhang, and Z.-S. Zhao, "Higher order sliding mode control with self-tuning law based on integral sliding mode," *IET Control Theory Appl.*, vol. 4, no. 7, pp. 1282–1289, Jul. 2010.
[37] Q. Zong, J. Wang, and Y. Tao, "Adaptive high-order dynamic sliding mode control for a flexible air-breathing hypersonic vehicle," *Int. J. Robust Nonlinear Control*, vol. 23, no. 15, pp. 1718–1736, Jul. 2013.
[38] P. Li, X. Yu, and B. Xiao, "Adaptive quasi-optimal higher order sliding-mode control without gain overestimation," *IEEE Trans. Ind. Informat.*, vol. 14, no. 9, pp. 3881–3891, Sep. 2018.
[39] Y. Ding, X. Wang, Y. Bai, and N. Cui, "Robust fixed-time sliding mode controller for flexible air-breathing hypersonic vehicle," *ISA Trans.*, vol. 90, pp. 1–18, Jul. 2019.
[40] S. P. Bhat and D. S. Bernstein, "Geometric homogeneity with applications to finite-time stability," *Math. Control, Signals, Syst.*, vol. 17, no. 2, pp. 101–127, May 2005.
[41] Y. Zhang, S. Tang, and J. Guo, "Adaptive-gain fast super-twisting sliding mode fault tolerant control for a reusable launch vehicle in reentry phase," *ISA Trans.*, vol. 71, pp. 380–390, Nov. 2017.
[42] C. Edwards and Y. B. Shtessel, "Adaptive continuous higher order sliding mode control," *Automatica*, vol. 65, pp. 183–190, Mar. 2016.
[43] C. Edwards and Y. Shtessel, "Adaptive dual-layer super-twisting control and observation," *Int. J. Control*, vol. 89, no. 9, pp. 1759–1766, Jun. 2016.
[44] Q. Hu and B. Xiao, "Fault-tolerant sliding mode attitude control for flexible spacecraft under loss of actuator effectiveness," *Nonlinear Dyn.*, vol. 64, nos. 1–2, pp. 13–23, Oct. 2010.
[45] J. Shaughnessy, S. Pinckney, and J. McMinn, *Hypersonic Vehicle Simulation Model: Winged-Cone Configuration*. Hampton, VA, USA: NASA Technical Memorandum, Nov. 1990.

FUHUI GUO received the bachelor's degree in control science and engineering from Tianjin Polytechnic University, Tianjin, China, in 2011, and the master's degree in 2015. She is currently pursuing the Ph.D. degree with the School of Automation, Beijing Institute of Technology, Beijing, China. Her research interests include the sliding mode control and attitude control, and robust and nonlinear control.

PINGLI LU received the B.S. degree in automation and the M.S. degree in control theory and engineering from Yanshan University, Qinhuangdao, China, in 2001 and 2004, respectively, and the Ph.D. degree in general and fundamental mechanics from Peking University, Beijing, China, in 2008. She is currently an Associate Professor with the School of Automation, Beijing Institute of Technology, Beijing. Her research interests include consensus control for multi-agent systems, attitude control, and robust and nonlinear control.